5-20-2005

Fine Structure of Beta Decay Endpoint Spectrum

Joseph Schechter
Syracuse University

Samina S. Masood
SUNY Oswego

Salah Nasri
University of Maryland - College Park

Fine structure of beta decay endpoint spectrum

Samina S. Masood*
Department of Earth Sciences, SUNY Oswego, Oswego, NY 13126

Salah Nasri†
Department of Physics, University of Maryland, College Park, MD 20742-4111,

Joseph Schechter‡
Department of Physics, Syracuse University, Syracuse, NY 13244-1130
(Dated: May 2005)

We note that the fine structure at the endpoint region of the beta decay spectrum is now essentially known using neutrino oscillation data, if the mass of one neutrino is specified. This may help to identify the effects of nonzero neutrino masses in future experiments. We also give a compact description of the entire range of allowed neutrino masses as a function of the third neutrino mass, m_3. A three neutrino assumption is being made. An exact treatment of phase space kinematics is used, in contrast to the conventional approximate formula. This work is independent of theoretical models; however, additional restrictions due to the assumption of a "complementary ansatz" for the neutrino mass matrix are also discussed. The ansatz implies that the values of the three neutrino masses should approximately be able to form a triangle. It is noted that most of the presently allowed neutrino mass sets have this triangular property.

PACS numbers: 14.60 Pq, 13.20 -v, 13.15 +g

I. INTRODUCTION

Measurement of the maximum electron energy in beta decay processes is the original approach [1] to finding the absolute value of a possible neutrino mass. It is still a subject of great interest [2] and may yield the first direct measurement of this crucial quantity. Especially interesting is the process of tritium decay [3, 4],

$$^3H \rightarrow {}^3He^+ + e^- + \bar{\nu}_e. \tag{1}$$

In this paper, we discuss how results obtained from present neutrino oscillation experiments [5] yield characteristic shapes for the beta decay endpoint spectrum which could help in signal identification [6]. The main point is that the present oscillation data already predict fairly reliably a bi-unique description of the shape of the endpoint spectrum if the mass of any neutrino is specified. This fortunate situation arises since, as we will discuss, the only unknown mixing angle is strongly bounded and hence cannot have much effect on the endpoint spectrum shape. So, running over the possible values of the third neutrino mass m_3, we would get a "catalog" of shapes which can be compared with the experimental shape to find a best fit. Of course, there are a number of practical corrections to the observed end point spectrum other than just the phase space and neutrino mixing effects to be considered here. These include [7] (i) Different final masses of $^3He^+$ due to different final atomic electron states, (ii) Corrections due to binding of ^3H in a molecule, (iii) Resolution function of the detector, (iv) Final state effects. The corrections should be made on each "page" of the catalog obtained.

We start in section II with an exact numerical treatment of the phase space, which contains a relevant correction to the approximate treatment often used. In section III we show that, as m_3 decreases from about the highest value considered to be consistent with information from cosmology, there are, in general, two solutions: type I where m_3 is the largest of the neutrino masses and type II where m_3 is the smallest of all the neutrino masses. Below about $m_3 = 0.052$ eV only the type II solutions are allowed. A characteristic feature is that the neutrinos 1 and 2 are extremely close in mass; their splittings range from about a ten thousandth of an eV to a hundredth of an eV. The end point spectrum shapes, showing the slope discontinuities corresponding to the vanishing of each neutrino's contribution, are plotted to illustrate these features. With a very great accuracy that might be achieved in the future,

*Electronic address: smasood@phy.syr.edu
†Electronic address: snasri@physics.umd.edu
‡Electronic address: schechte@phy.syr.edu

the spacings of the neutrinos could conceivably survive the needed corrections mentioned above. However the most practical procedure would probably be to integrate each corrected predicted spectrum shape (of definite m_3 and type) over an energy interval and then look to see which one is best fit by the experimental value.

In section IV we discuss some model restrictions on the ranges of m_3 which lead to type I and type II solutions. These restrictions arise by assuming a so-called "complementary ansatz" for the neutrino mass matrix. The observation of m_3 in the non-allowed ranges would constitute a falsification of the ansatz.

Finally, section V contains a brief summary and some discussion.

II. PHASE SPACE KINEMATICS

Taking the tritium decay example and assuming one massive neutrino for the time being, let M be the mass of the tritium atom, M' the mass of $^3He^+$, m_e the electron mass and m_ν the neutrino mass. Often [8], the kinetic part of the recoil nucleus energy is neglected so one has an easy approximate formula for the maximum electron energy:

$$E_{max}(approx) = M - M' - m_\nu. \tag{2}$$

The exact formula, corresponding to the physical situation where the neutrino and the recoil nucleus both emerge with the same velocity is

$$E_{max} = \frac{1}{2M}[M^2 + m_e^2 - (m_\nu + M')^2]. \tag{3}$$

To get an idea of the accuracy of the approximate formula we use [9] the input masses (in MeV):

$$M = 2809.431935572 \qquad\qquad M' = 2808.902399642, \tag{4}$$

to obtain Table I. Notice that in Eq. (4) we have, for the purpose of conveniently "tracking" digits in this illustration, included more digits than warranted for the experimental accuracy of M and M'.

m_ν(eV)	E_{max}(MeV)	δE_{max}(eV)
10	0.5295225	3.431
1	0.529531497	3.433
0.1	0.529532397	3.433
0.01	0.529532487	3.433
0.001	0.529532496	3.433

TABLE I: Comparison of exact and approximate maximum electron energy for different neutrino masses. Note that $\delta E_{max} = E_{max}(approx) - E_{max}$.

In the second column of Table I, as one goes to lower neutrino masses the change in the maximum electron energy occurs, as expected, in the decimal place corresponding to the neutrino mass. The third column shows that there is a correction to the approximate formula Eq.(2) of 3.43 eV which is essentially independent of neutrino mass. This value is considerably larger than (as we will review) the still allowed values of neutrino mass and hence is very relevant. Its analytic form may be obtained by subtracting Eq.(3) from Eq.(2) and then neglecting the neutrino mass dependence:

$$\delta E_{max} = E_{max}(approx) - E_{max} \approx \frac{1}{2M}[(M - M')^2 - m_e^2]. \tag{5}$$

Since one gets a decent approximation to E_{max} by subtracting the (neutrino mass independent) expression for δE_{max} just given from $E_{max}(approx)$, the difference of any two maximum electron energies essentially equals minus the difference of the corresponding neutrino masses.

Considering that there is a relevant correction to the approximate end point formula, it seems prudent to also calculate the phase space factor exactly. This does not seem to have been used before but is straightforward to get by standard methods [10]. We write the distribution in the electron energy, E as,

$$|\frac{d\Gamma}{dE}| = \frac{1}{(2\pi)^3}\frac{|\mathcal{M}|^2}{(2M)^2}\Phi(E), \tag{6}$$

where $|\mathcal{M}|^2$ stands for a suitably spin averaged squared amplitude and $\Phi(E)$ is the desired phase space factor. After integration over one coordinate of the Dalitz diagram, we find:

$$\begin{aligned}\Phi(E) &= \sqrt{(E_2^{*2} - M'^2)(E_3^{*2} - m_e^2)},\\ E_2^* &= \frac{m_{12}^2 - m_\nu^2 + M'^2}{2m_{12}},\\ E_3^* &= \frac{M^2 - m_{12}^2 - m_e^2}{2m_{12}},\\ m_{12} &= \sqrt{M^2 + m_e^2 - 2ME}.\end{aligned} \tag{7}$$

In carrying out the integration we assumed that there is a negligible energy dependence introduced from $|\mathcal{M}|^2$. This is reasonable since we are only interested in the very small endpoint region. The shape of Φ in the endpoint region is illustrated in Fig. 1 for the case of a one electron volt neutrino.

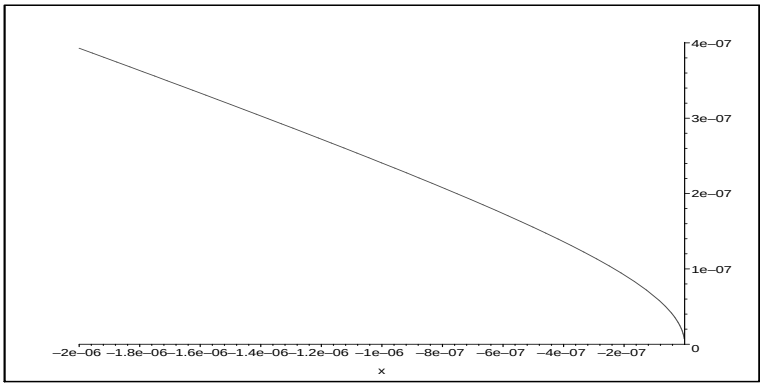

FIG. 1: Plot of the phase space factor Φ for a 1 eV neutrino. $x = E - Emax$ has units of MeV while Φ has units of MeV^2

III. CASE OF THREE NEUTRINOS

In the realistic three neutrino case, the ordinary beta decays actually correspond to decays with different weights into three neutrinos of different mass. The effective phase space factor is:

$$\Phi_{eff}(E) = \sum_{i=1}^{3} |K_{1i}|^2 \Phi_i(E)\theta(E_{max,i} - E), \tag{8}$$

where $\Phi_i(E)$ is the phase space factor and $E_{max,i}$ the maximum electron energy for a neutrino of mass m_i. The K_{1i} are matrix elements of the lepton mixing matrix, displayed for convenience in the Appendix. Notice that no CP phases contribute.

As the result of a number of beautiful experiments [5], there is now a great deal of information available about the squared mass differences and mixing angles involved in neutrino physics. Essentially, assuming that the three neutrino scenario is correct, if the absolute mass of any one neutrino is specified, everything in Eq. (8) up to a possible two-fold ambiguity is known with useful accuracy. According to a recent analysis [11] it is possible to extract from the data to good accuracy, two squared neutrino mass differences: $m_2^2 - m_1^2$ and $|m_3^2 - m_2^2|$, and two inter-generational mixing angle squared sines: s_{12}^2 and s_{23}^2. Furthermore the inter-generational mixing parameter s_{13}^2 is found to be very small. Specifically, we will adopt,

$$\begin{aligned}A \equiv m_2^2 - m_1^2 &= 6.9 \times 10^{-5} eV^2,\\ B \equiv |m_3^2 - m_2^2| &= 2.6 \times 10^{-3} eV^2.\end{aligned} \tag{9}$$

The uncertainty in these determinations is roughly 25%. Similarly for definiteness we will adopt the best fit values for s_{12}^2 and s_{23}^2 obtained in the same analysis:

$$s_{12}^2 = 0.30, \quad s_{23}^2 = 0.50. \tag{10}$$

These mixing parameters also have about a 25% uncertainty. The experimental value of s^2_{13} was less accurately determined. At present only the 3 σ bound,

$$s^2_{13} \leq 0.047, \tag{11}$$

is available and we will choose, for definiteness, $s^2_{13} = 0.04$. Then, our values for the weighting coefficients in Eq. (8) will be taken as,

$$\begin{aligned} |K_{11}|^2 &= (c_{12}c_{13})^2 = 0.672, \\ |K_{12}|^2 &= (s_{12}c_{13})^2 = 0.288, \\ |K_{13}|^2 &= (s_{13})^2 = 0.040. \end{aligned} \tag{12}$$

Future improvements in these factors are not expected to make qualitative changes in the endpoint spectrum shapes. In particular, even though the exact value of $|K_{13}|^2$ is not known, the bound of Eq.(11) guarantees that the contribution of neutrino three will be no larger than the amount to be given.

The goal would be to fit the endpoint spectrum shape observed in a future tritium decay experiment to one of the family of shapes that we can now find by running through the possible values of the third neutrino mass, m_3. For a given value of m_3 one can obtain from Eqs.(9) two different solutions for the other masses m_1 and m_2. We call the solution where m_3 is the largest neutrino mass, the type I case. The case where m_3 is the smallest neutrino mass is designated type II. m_1 will be determined from the assumed value of m_3 as,

$$m_1^2 = m_3^2 - A \mp B, \tag{13}$$

where the upper and lower sign choices respectively refer to the type I and type II cases. In either case we find m_2 as,

$$m_2^2 = A + m_1^2. \tag{14}$$

Which values of m_3 are allowed? A recent cosmology bound [12] based on structure formation requires,

$$m_1 + m_2 + m_3 < 0.7 \text{ eV}. \tag{15}$$

Thus values of m_3 greater than about 0.3 eV are physically disfavored. However, it seems extremely important that this bound be verified independently by laboratory experiments like tritium beta decay. At the lower end, we see from Eq.(13) that the type I solutions must satisfy,

$$m_3 > \sqrt{A + B} \approx 0.0517\text{eV}. \tag{16}$$

On the other hand, the type II solutions need only obey $m_3 > 0$ at the lower end. Some typical allowed solutions are shown in Table II.

type	m_1(eV)	m_2(eV)	m_3(eV)
I	0.2955	0.2956	0.3
II	0.3042	0.3043	0.3
I	0.0856	0.0860	0.1
II	0.1119	0.1123	0.1
I	0.0305	0.0316	0.06
II	0.0783	0.0787	0.06
I	0.0000	0.0083	0.0517
II	0.0643	0.0648	0.04
II	0.0541	0.0548	0.02
II	0.0506	0.0512	0.005
II	0.0503	0.0510	0.001

TABLE II: Typical solutions for (m_1, m_2) as m_3 is lowered from about the highest value which is experimentally reasonable. In the type I solutions m_3 is the largest mass while in the type II solutions m_3 is the smallest mass.

This table contains a great deal of information in a very small space. For orientation, we remark that the type I situation is usually called the "normal hierarchy" while the type II situation is usually called the "inverted hierarchy". Actually the table shows that over a large portion of the currently favored neutrino mass range (i.e. roughly from m_3 =0.1 to 0.3 eV as opposed to $m_3 = 0$ to 0.1 eV) and for either type I or type II, the neutrino mass spectrum is

better described as an almost degenerate situation rather than one involving a hierarchy. If one goes above $m_3 = 0.3$ eV the degeneracy is even enhanced. Below about $m_3 = 0.1$ hierarchies can exist. Note that the maximum ratio associated with a normal hierarchy corresponds to m_3/m_2 only about 6 and is achieved just when (while decreasing m_3) this type vanishes. On the other hand, we see that the ratio m_2/m_3 can become indefinitely large (as m_3 goes to zero) for the inverted hierarchy case. Another interesting feature shown in this table is the near mass degeneracy of neutrinos one and two for all the solutions. The table precisely shows how this near degeneracy gets somewhat relaxed as the mass m_3 decreases from the top allowed value. Finally, the table illustrates the vanishing of the type I solutions, consistently with Eq. (16), as m_3 is decreased.

Now let us examine the endpoint spectrum shape computed from Eq. (8). Figure 2 shows the endpoint spectrum in the type I case where $m_3 = 0.3$ eV and correspondingly $m_1, m_2 = 0.2955, 0.2956$ eV. In addition to the vanishing of Φ_{eff} at $x = E - E_{max,1} = 0$ due to neutrino one there is also a nearby discontinuity of slope at $x = E_{max,2} - E_{max,1}$ due to neutrino two. The presence of two distinguishing features may be easier to recognize than just one alone. However, the difference between these two points is read off to be about one ten-thousandth of an eV (which, as remarked previously, also is the difference between the two neutrino masses seen in Table II). This seems to be a rather small number for experimental detection. The slope discontinuity due to neutrino three is still further to the left and is shown, greatly magnified, in Fig. 3. It is only about five one thousandths of an eV away from the others. However the signal for neutrino three is suppressed by the small value of s^2_{13}, as discussed above. Conceivably, requiring the presence of three distinguished points together may make the neutrino mass signal somewhat easier to recognize in the future.

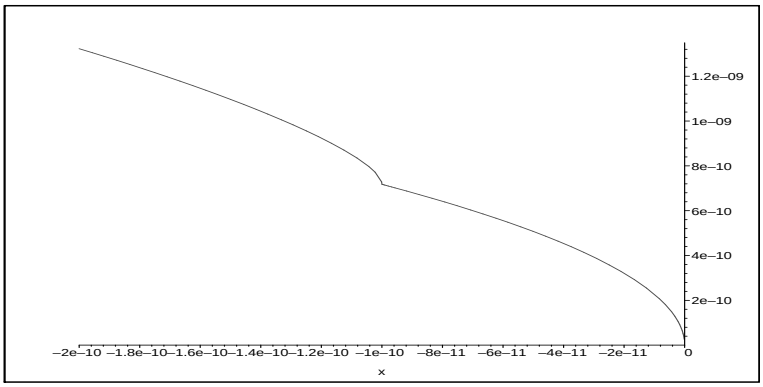

FIG. 2: Plot of Φ_{eff} for $m_3 = 0.3eV$ and $m_1, m_2 = 0.2955, 0.2956eV$ in the region showing the m_1, m_2 structure. $x = E - E_{max,1}$ has units of MeV while Φ_{eff} has units of MeV^2

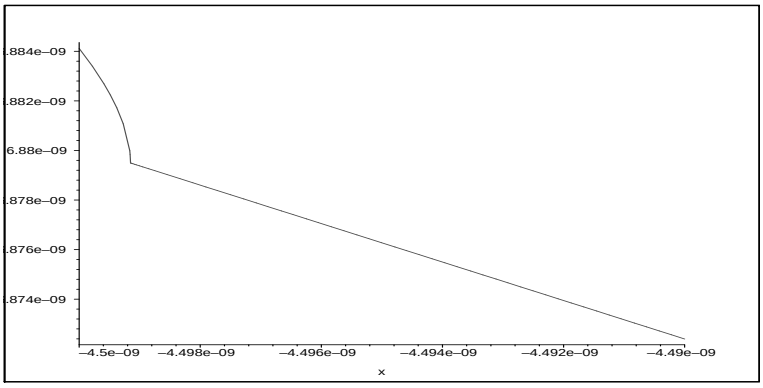

FIG. 3: Plot of Φ_{eff} for $m_3 = 0.3eV$ and $m_1, m_2 = 0.2955, 0.2956eV$ in the region showing the m_3 structure. $x = E - E_{max,1}$ has units of MeV while Φ_{eff} has units of MeV^2

The endpoint spectrum for the type II solution with $m_3 = 0.3$ eV is similarly plotted in Figs. 4 and 5. For this case, since m_3 is the smallest mass, one recognizes that the curve in Fig. 4 does not quite vanish at the right end (larger electron energy) but goes to a small value controlled by the small value of s_{13}. Clearly, as discussed above, finding a more accurate value of K_{13} consistent with the experimental bound will have a small effect on the endpoint spectrum shape. The actual vanishing at the right end is shown, magnified, in Fig. 5. The spacings between the various neutrino points are essentially the same in magnitude as in the type I case. However the type I and II cases can, in principle, be distinguished by noting that the long interval comes first in the type II case.

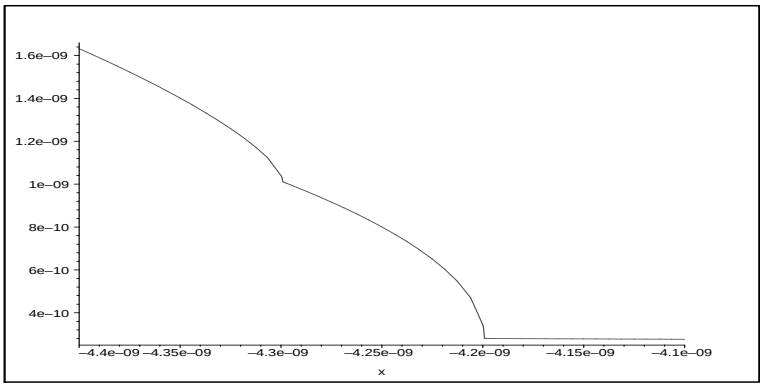

FIG. 4: Plot of Φ_{eff} for $m_3 = 0.3eV$ and $m_1, m_2 = 0.3042, 0.3043eV$ in the region showing the m_1, m_2 structure. $x = E - E_{max,3}$ has units of MeV while Φ_{eff} has units of MeV^2

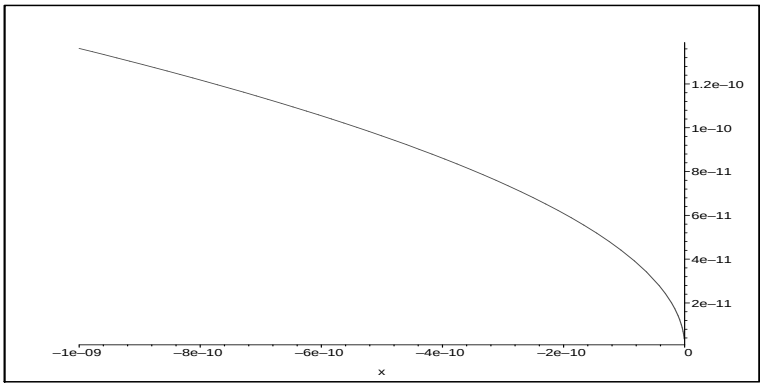

FIG. 5: Plot of Φ_{eff} for $m_3 = 0.3eV$ and $m_1, m_2 = 0.3042, 0.3043eV$ in the region showing the m_3 structure. $x = E - E_{max,3}$ has units of MeV while Φ_{eff} has units of MeV^2

The figures for lower values of m_3 are very similar in shape. We give one more plot here for comparison. As m_3 decreases, the distinguishing points for neutrinos one and two move somewhat apart. This can be understood since the corresponding masses are seen in Table II to move apart and, according to Eqs. (2) and (5) the splitting of the maximum electron energies is, to a very decent approximation, the same as the neutrino mass splitting. In Fig. 6 the type I case with $m_3 = 0.06$ eV is shown. Here the splitting between the neutrino one and two points is one order of magnitude larger than for the corresponding Fig. 2. The splitting between the neutrino three point and the others is boosted to about three hundreths of an eV.

Evidently, it may be sometime in the future before the accuracy of the beta decay experiments enables one to see all the details of the fine structure displayed here. The present approach may nevertheless be useful in the near future for numerically computing the integrated spectrum as a function of both an energy interval Δ as well as the running parameter m_3 and searching for a best fit to experiment. This would have to be done for both the type I and type II cases. A clear best fit would, in principle, determine all three neutrino masses in a manner consistent with the neutrino oscillation data. Of course, the other corrections mentioned in the Introduction (which are beyond the scope of the present paper) must be included too. In the literature [6] there has been some debate about the proper choice of an effective neutrino mass to replace all three masses in the analysis of endpoint experiments. Clearly the procedure suggested here would enable one to measure the effectiveness of different choices. A more detailed discussion of this aspect will be given elsewhere.

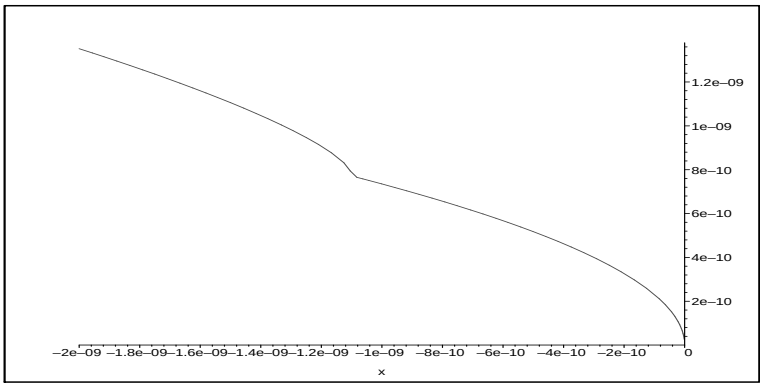

FIG. 6: Plot of Φ_{eff} for $m_3 = 0.06eV$ and $m_1, m_2 = 0.0305, 0.0316eV$ in the region showing the m_1, m_2 structure. $x = E - E_{max,1}$ has units of MeV while Φ_{eff} has units of MeV^2

IV. RESTRICTIONS FROM A "COMPLEMENTARY" ANSATZ

Up to now we have considered only experimental inputs. A key feature was allowing m_3 to vary in order to run through a family of endpoint spectrum shapes which might be compared with future experiments. A similar procedure was recently followed in order to derive consequences from an ansatz [13]-[18] which allows one to compute (in case the neutrinos are of Majorana type) the two Majorana CP violation phases, given m_3 and the Dirac phase δ. That"complementary ansatz" specifies that the trace of the prediagonal 3×3 neutrino mass matrix vanishes (in a charged lepton diagonal basis wherein non-physical phases are appropriately chosen). Since the prediagonal neutrino mass matrix is complex, the vanishing trace gives two physical conditions. Taking $A, B, s^2_{12}, s^2_{23}, s^2_{13}$ as "known", running through the two parameters m_3 and the Dirac CP phase δ then determines the allowed values of the two Majorana CP phases. This gives a two parameter family of solutions for the complete set of neutrino parameters.

Now in carrying out this analysis, the starting point was Eqs. (13) and (14) above. However it turns out that the allowed ranges of m_3 are more restrictive than those obtained in and after Eq. (16). In Table III, taken from ref. [18], it can be seen that the smallest allowed value of m_3 for type I solutions is in the range $0.058 - 0.059$ eV rather than 0.0517 eV as found here. Similarly, the smallest allowed value of m_3 for type II solutions is in the range $0.00068 - 0.00246$ eV rather than zero as obtained here. The range of minima exists because there is some dependence on the input Dirac phase δ.

type	$(m_3)_{min}$ $(\delta = 0)$ in eV	$(m_3)_{min}$ $(\delta = 0.5)$	$(m_3)_{min}$ $(\delta = 1.0)$	$(m_3)_{min}$ $(\delta = 1.5)$	$(m_3)_{min}$ $(\delta = 2.0)$	$(m_3)_{min}$ $(\delta = 2.5)$
I	0.0592716	0.0590967	0.0587178	0.0584799	0.0586203	0.0589971
II	0.0006811	0.00105461	0.0019024	0.0024636	0.0021294	0.0012723

TABLE III: Minimum allowed value of the input mass, m_3 as a function of the input CP violation phase, δ for type I and II solutions using the "complementary" ansatz. Here, the choice $s^2_{13} = 0.04$ has been made.

It may be amusing to see why the ansatz leads to more restrictions. Take the simplified case, treated in detail in ref. [16], where $\delta = 0$. Then the ansatz condition amounts to the lengths corresponding to the three neutrino masses forming a triangle in the complex plane. (The two independent Majorana phases are related to the internal angles of this triangle). The procedure outlined here obtains, for a given assumed value of m_3, the three neutrino masses. However it is not guaranteed that they form a triangle, since the mass of one neutrino may be greater than the sum of the masses of the two others. The case where $m_3 = 0.0517$ in Table II is an obvious example of this situation. In the case when δ is non-zero, treated in detail in ref. [18], there is also a triangle condition but the triangle is not made simply using the masses as sides. At the present moment, the "non-triangular" regions of m_3 space constitute a small, but interesting, part of the allowed range (considering of course the type I and type II cases separately). The allowed regions are summarized in Figs. 7 and 8 . So, if in the future, the neutrino masses are found from an endpoint spectrum analysis to give (assuming suitably updated numbers) m_3 outside the range predicted by the complementary ansatz, the latter can be ruled out.

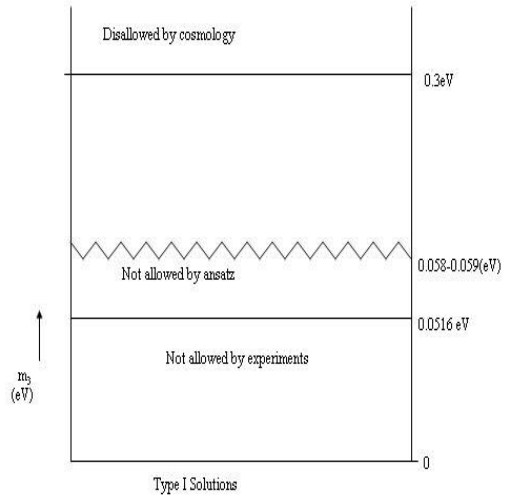

FIG. 7: Schematic view of the allowed range of neutrino mass m_3 for the type I solution. The wiggly line illustrates the restrictions on the allowed range due to assuming the complementary ansatz for the neutrino mass matrix.

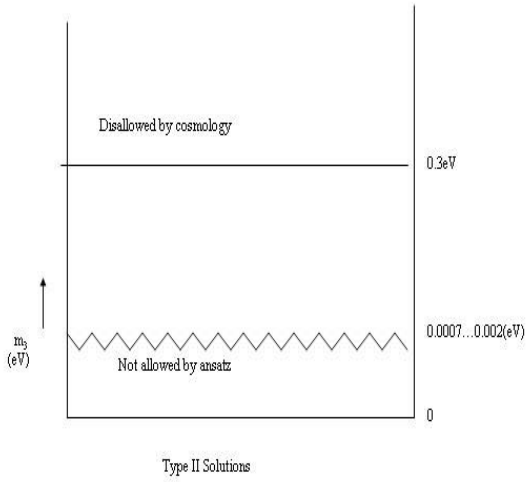

FIG. 8: Schematic view of the allowed range of neutrino mass m_3 for the type II solution.

V. SUMMARY AND DISCUSSION

We have demonstrated that, given the value of the third neutrino mass m_3, the endpoint spectrum of the electron energy in beta decay is biuniquely predicted to a reasonable approximation using the experimental results on neutrino oscillations and their analyses. For definiteness some characteristic endpoint spectrum shapes were explicitly illustrated. This seems important not only as an indication of how much our understanding of neutrinos has advanced in the last ten years but as a convenient benchmark for helping to analyze future beta decay experiments. Of course the actual experimental results require other important corrections to this "ideal" theoretical picture. Some novel features of this paper which may be of interest include:

1. While the kinematics of the endpoint spectrum has been discussed many times in the literature, the exact formula for the phase space dependence on the electron energy (obtained by performing one integration over the Dalitz diagram while holding the invariant matrix element constant), Eq. (7), does not seem to have been previously used. These results may not make big changes in other analyses but one can use them with confidence since there will then be no question of kinematical (nucleon recoil) corrections needing to be separately taken into account.

2. The method of analysis of the presently allowed neutrino masses using the squared mass differences obtained from the neutrino oscillation experiments presented in section III involves listing the results for the masses of neutrinos one and two while choosing various values of the mass m_3. The cases where m_3 is heaviest (type I) and where it is lightest (type II) are treated separately. For example, as discussed in section III, one sees that the currently allowed neutrino mass spectrum is characterized for a large part of its range as almost degenerate rather than hierarchical. The main point is that for any choice of m_3 and type, the shape of the endpoint spectrum is already pretty well known from the neutrino oscillation experiments. Even though the value of s^2_{13} is only bounded, it will not affect the shape much. Our treatment easily shows that the slope discontinuities corresponding to the mass differences of individual neutrinos occur very close to each other. That would make detailed verification of the shape difficult in the near future. However, knowing the shape for any value of m_3 makes it possible to integrate the final electron distribution over an energy interval Δ corresponding to a given experiment. Then the number of predicted electrons could be plotted as a function of m_3 and Δ to get an "ideal" estimate of the experimental sensitivity to distinguishing different neutrino mass scenarios. This ideal estimate should of course be corrected for effects mentioned in section I, but that is beyond the scope of the present paper. Further applications of this approach will be presented elsewhere.

3. The complementary ansatz for the neutrino mass matrix [13]-[18] enables one to predict, given m_3 and the "Dirac" CP phase, the two Majorana phases of the lepton mixing matrix. It is of interest because it enables the estimation of the neutrinoless double beta decay quantity m_{ee} and, in a certain model, the baryon asymmetry by the leptogenesis mechanism without making arbitrary assumptions about these phases. An amusing feature of the ansatz is that (to the approximation that the effect of the Dirac CP phase δ is negligible) the magnitudes of the three neutrino masses must make up a triangle. If they don't, the ansatz would be falsified. In section IV, the regions of allowed neutrino masses which falsify the ansatz were specified (including the effect of δ). It was pointed out that a large portion of the currently allowed range of m_3 actually does correspond to a triangular pattern of neutrino masses. However, the small non-triangular region near $m_3 = 0.0517$ eV is the only place where m_3 is several times higher than m_2.

Acknowledgments

We are grateful to Mariam Tortola for checking our equations and correcting an overall factor in Eq. (6). S.S.M would like to thank the Physics Department at Syracuse University for their hospitality. The work of S.N is supported by National Science foundation grant No. PHY-0099. The work of J.S. is supported in part by the U. S. DOE under Contract no. DE-FG-02-85ER 40231.

APPENDIX A: LEPTON MIXING MATRIX

A symmetrical parameterization of the lepton mixing matrix, K can be written as:

$$K = \begin{bmatrix} c_{12}c_{13} & s_{12}c_{13}e^{i\phi_{12}} & s_{13}e^{i\phi_{13}} \\ -s_{12}c_{23}e^{-i\phi_{12}} - c_{12}s_{13}s_{23}e^{i(\phi_{23}-\phi_{13})} & c_{12}c_{23} - s_{12}s_{13}s_{23}e^{i(\phi_{12}+\phi_{23}-\phi_{13})} & c_{13}s_{23}e^{i\phi_{23}} \\ s_{12}s_{23}e^{-i(\phi_{12}+\phi_{23})} - c_{12}s_{13}c_{23}e^{-i\phi_{13}} & -c_{12}s_{23}e^{-i\phi_{23}} - s_{12}s_{13}c_{23}e^{i(\phi_{12}-\phi_{13})} & c_{13}c_{23} \end{bmatrix}. \quad \text{(A1)}$$

Some advantages of this choice are discussed in sections V and VI of [18]. As written, it holds for the case of Majorana type neutrinos. There are three CP violating phases, ϕ_{12}, ϕ_{23} and ϕ_{13}. The "invariant" combination $\delta = \phi_{12}+\phi_{23}-\phi_{13}$

corresponds to the "Dirac phase". If neutrinos are of Dirac type, only a single phase (say ϕ_{13}) may be taken to be non-zero.

---

[1] E. Fermi, Z. Physik, **88**, 161 (1934).
[2] For a review, see C. Aalseth et al, arXiv:hep-ph/0412300.
[3] C. Weinheimer et al, Nucl. Phys. B (Proc. Suppl.)**118**, 279 (2003); Ch. Kraus et al, arXiv:hep-ex/0412056.
[4] V. Lobashev et al, Nucl. Phy. B (Proc. Suppl.)**91**, 280 (2001).
[5] KamLAND collaboration, K. Eguchi et al, Phys. Rev. Lett. **90**, 021802 (2003); SNO collaboration, Q. R. Ahmad et al, arXiv:nucl-ex/ 0309004; K2K collaboration, M. H. Ahn et al, Phys. Rev. Lett. **90**, 041801 (2003); For recent reviews see, for examples, S. Pakvasa and J. W. F. Valle, special issue on neutrino, Proc. Indian Natl. Sci. Acad. Part A **70**, 189 (2004) [arXiv:hep-ph/0301061] and V. Barger, D. Marfatia and K. Whisnant, Int. J. Mod. Phys. E **12**, 569 (2003)[arXiv:hep-ph/0308123].
[6] Relevant discussions are given by R. E. Shrock, Phys. Lett. B **96**,159 (1980); F. Vissani, arXiv:hep-ph/0102235; Y. Farzan, O. L. G. Peres and A. Yu. Smirnov, Nucl. Phys. B **612**, 59 (2001); J. Studnik and M. Zralek, arXiv:hep-ph/0110232; F. Feruglio, A. Strumia and F. Vissani, Nucl. Phys. B **637**, 345 (2002); Y. Farzan and A. Yu. Smirnov, Phys. Lett. B **557**, 224 (2003); S. M. Bilenky, C. Giunti, J. A. Grifols and E. Masso, Phys. Rep. **379**, 69 (2003).
[7] These are discussed in chap. 2 of F. Boehm and P. Vogel, Physics of massive neutrinos, Cambridge Univ. press (1987). For more recent work, see S. Gardner, V. Bernard and U.-G. Meissner, Phys. Lett. B **598**, 188 (2004) and L. Platter, H.-W. Hammer and U.-G. Meissner, Phys. Lett. B **254** (2005).
[8] Of course, in recent high accuracy experiments like the works of [3] and [4] above, recoil corrections are either approximated or the end point energy is treated as a fitting parameter.
[9] WWW Table of Atomic Masses, http://ie.lbl.gov/toi2003/MassSearch.asp. We have included the electron mass correction and the lowest Bohr energy for the Helium ion.
[10] See for example page 298 of Particle Data Group, Phys. Letts. B **592**, 1 (2004).
[11] M. Maltoni, T. Schwetz, M. A. Tortola and J. W. F. Valle, Phys. Rev. D **68**, 113010 (2003). For the choice $m_2 > m_1$ see A. de Gouvea, A. Friedland and H. Murayama, Phys. Lett. **B490**, 125 (2000).
[12] D. N. Spergel et al, Astrophys. J. Suppl. **148**: 175 (2003); S. Hannestad, JCAP **0305**: 004 (2003).
[13] D. Black, A. H. Fariborz, S. Nasri and J. Schechter, Phys. Rev. **D62**, 073015 (2000).
[14] X.-G. He and A. Zee, Phys. Rev. **D68**, 037302, (2003).
[15] W. Rodejohann, Phys. Lett. **B579**, 127 (2004).
[16] S. Nasri, J. Schechter and S. Moussa, Phys. Rev. **D70**, 053005 (2004).
[17] S. Nasri, J. Schechter and S. Moussa, Int. J. Mod. Phys. A, **19** No. 31, 5367 (2004), Proc. of MRST 2004 conference, M. Frank and C. S. Kalman, editors [arXiv:hep-ph/0406243].
[18] S. S. Masood, S. Nasri and J. Schechter, Phys. Rev. D, **71**,093005 (2005) [arXiv: hep-ph/0412401].